Open access • Journal Article • DOI:10.1051/JPHYSCOL:1975138

Poiseuille flow instabilities in nematics — Source link

E. Guyon, E. Guyon, Pawel Pieranski

Institutions: University of Paris-Sud, University of California, Los Angeles

Published on: 01 Mar 1975 - Le Journal De Physique Colloques (EDP Sciences)

Topics: Hagen–Poiseuille equation, Shear flow, Velocity gradient and Body force

POISEUILLE FLOW INSTABILITIES IN NEMATICS

E. Guyon, P. Pieranski

JOURNAL DE PHYSIQUE Colloque C1, supplément au n° 3, Tome 36, Mars 1975, page C1-203

Classification
Physics Abstracts
7.130 — 6.350

POISEUILLE FLOW INSTABILITIES IN NEMATICS (*)

E. GUYON (**) and P. PIERANSKI (***)

Laboratoire de Physique des Solides, Université Paris-Sud, 91405 Orsay, France

Résumé. — Nous avons étendu notre étude des instabilités de cisaillement dans les nématiques, alignés perpendiculairement à la vitesse et au gradient de vitesse au cas d'une géométrie de Poiseuille plane. Nous retrouvons les modes d'instabilité *homogène* et en *rouleaux*. Le tenseur des contraintes non uniforme donne naissance à des forces en volume qui changent la direction d'écoulement et sont couplées à la distorsion. Nous rendons compte aussi de structures nouvelles dues à la présence de distorsion au voisinage des deux faces limites. Un mode original de longueur d'onde variable est décrit.

Abstract. — We have extended our study of shear flow instabilities in nematics, aligned perpendicular to the velocity and velocity gradient, to the plane Poiseuille flow case. We recover the *homogeneous* as well as the *roll* instability modes. The non-uniform anisotropic stress tensor gives rise to body forces which deflect the flow lines and couple with the distortions. Novel structures are met due to the existence of distortions near both the upper and lower plates. A new variable-wavelenght linear mode is found.

1. **Introduction.** — During the last year we have reported [1, 2] a series of hydrodynamic instabilities met when an aligned nematic film of thickness d is sheared between two parallel plates if, in the undistorted state, the director $\mathbf{n}$ is perpendicular to both the velocity $\mathbf{v}$ and the velocity gradient. The geometry is given in figure 1.

A *first type* of instability corresponds to a uniform distortion and can be characterized by the values of the small components of the unit vector $\mathbf{n}$, n_y and n_z. The two possible equivalent distortions are given in the figure. This *homogeneous* mode is a linear instability : the distortion varies continuously and reversibly from zero ($n_y, n_z \ll 1$) when the shear rate s exceeds a critical value s_c. The threshold is given by a critical dimensionless Ericksen number [1, 3] :

$$\mathrm{Er}_c = \frac{\sqrt{\alpha_2\,\alpha_3}}{\sqrt{K_1\,K_2}}\,s_c\,d^2 = \pi^2 \qquad (1)$$

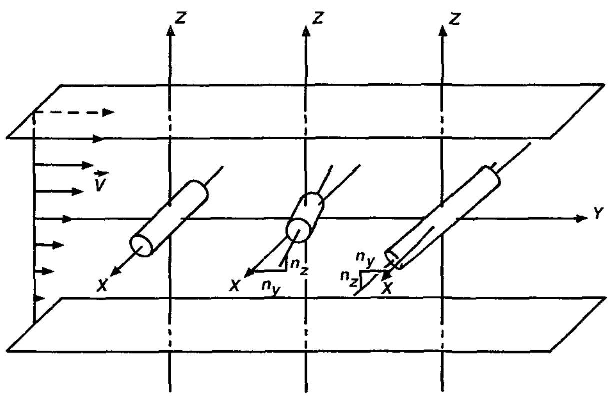

FIG. 1. — Shear flow instability in nematics. In the undistorted state on the left of the figure, the molecular orientation along x is perpendicular to the velocity and velocity gradient. The two possible equivalent distortions are indicated on the right of the figure.

K_1 and K_2 are the splay and twist elastic terms which appear due to the distortion and tend to restore the initial alignment due to the effect of the boundaries. The hydrodynamic torques, proportional to α_2 and α_3, act as soon as an initial fluctuation (n_y plus n_z) takes place and destabilize the initial state if the product $\alpha_2\,\alpha_3$ is positive [4].

The experiments reported as well as those described in (1) and (2) are done with MBBA where both $\alpha_2 \sim -1$ poise and $\alpha_3 \sim -0.008$ poise are negative [5, 6].

In a *second type* of instability met in particular when an alternating shear is applied, *rolls* of axis parallel to the velocity are formed. This linear mode involves a *focusing effect* where a vertical force appears due to the shear acting on the periodic distortion of the director, n_y and $n_z \propto \cos kx$ (with a wavelength $2\,\pi/k$ of the order of $2d$).

This article describes an extension to the Poiseuille flow geometry (Fig. 2). The flow takes place along y between two parallel plates. The initial alignment of the molecules fixed by the boundaries is again perpen-

(*) Supported in part by D. G. R. S. T.
(**) Also Physics Department, UCLA, Los Angeles, California 90024.
(***) This article is a part of a thesis to be presented at the University Paris-Sud.

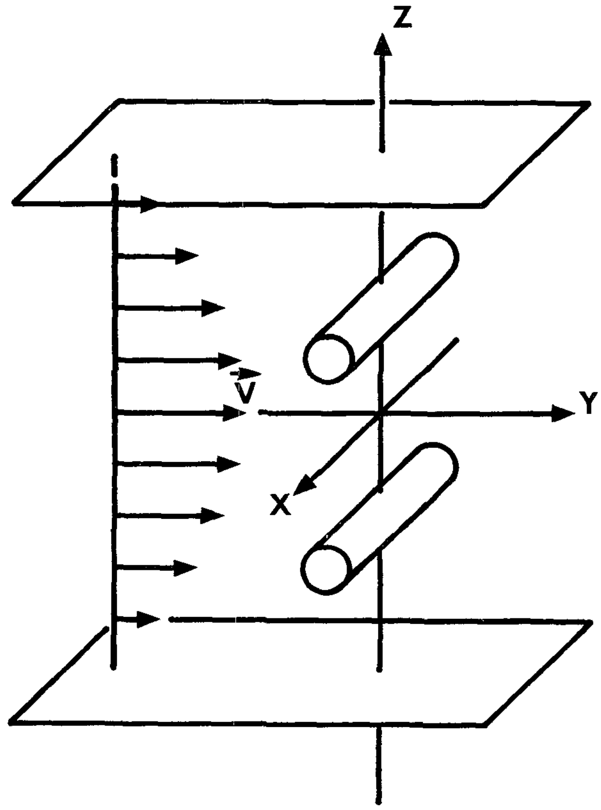

FIG. 2. — Undistorted state in the Poiseuille flow problem.

dicular to the velocity and velocity gradient. The velocity profile is parabolic and the pressure drop along y over the length L is

$$\Delta p = \eta L \frac{\mathrm{d}s}{\mathrm{d}z} .$$

The shear rate s is maximum near the limiting plates and the instability can be understood qualitatively as in the shear flow problem if we assume that, near the linear threshold, the distortions near the two plates are independent. Two types of solutions are expected (Fig. 3).

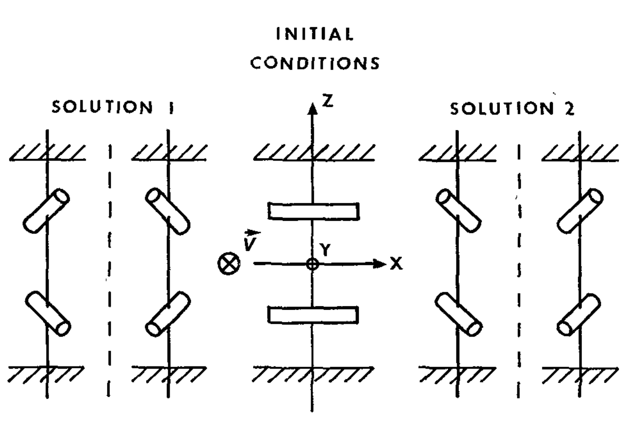

FIG. 3. — The four possible distortions in the Poiseuille flow geometry referred to in the text as solutions 1 and 2.

Solution 1.

$$n_y(z) = n_y(-z) , \qquad n_z(z) = -n_z(-z) .$$

This solution involves a finite average *twist* over the thickness.

Solution 2.

$$n_y(z) = -n_y(-z) , \qquad n_z(z) = n_z(-z) .$$

This one has an associated average *splay*.

Clearly one also has two other mirror solutions obtained by reflection through a yz plane. Thus we have *four* possible distorted states. In fact, above the threshold, nonlinear effects resulting in an interaction between the upper- and lower-half distorted structures are expected. These effects are beyond the present description.

The linear problem was first discussed by de Gennes [3]. He also obtained an equation for the threshold given by an Ericksen number

$$\mathrm{Er}_c = \frac{\sqrt{\alpha_2 \alpha_3}}{\eta \sqrt{K_1 K_2}} \frac{\Delta p_c}{L} \left(\frac{d}{2}\right)^3 \sim 12.5 . \qquad (2a)$$

The result can be written as

$$\mathrm{Er}_c = \frac{\sqrt{\alpha_2 \alpha_3}}{\sqrt{K_1 K_2}} \bar{s}_c \left(\frac{d}{2}\right)^2 \sim \frac{12.5}{2} \qquad (2b)$$

where $\bar{s}_c$ is the average shear acting over half the thickness ($d/2$). Under this form, the result is qualitatively similar to eq. (1).

Before getting into the description of the modes obtained experimentally, it is useful to describe independently two effects which play an essential role in the problem.

2. **Anisotropic stress tensor effects.** — EFFECT A. — We consider a Poiseuille flow between two parallel plates. Here the alignment of $\mathbf{n}$, fixed in the bulk by a large enough magnetic field, is practically undisturbed by the flow. If the molecules are in the plane of the plates and at an angle θ with the flow, one observes that [7] :

— a transverse pressure head of the same order of magnitude as the longitudinal one develops across the cell,

— the flow lines are deflected towards $\mathbf{n}$.

These effects are the largest for $\theta = \pi/4$ and vanish in the symmetrical configurations $\theta = 0$ and $\pi/2$. They are easily understood in terms of the Leslie Ericksen asymmetric stress tensor $\boldsymbol{\sigma}$ [8]. Due to the variation of the shear rate along z, the component $F_A = \partial\sigma_{zx}/\partial z$ gives a force along x which causes both effects. Note that in a shear flow, where s and σ_{zx} are uniform in space, no body force and, consequently, no such effects develop.

EFFECT B. — Even when the *shear is uniform, bulk* forces appear if the molecular orientation varies in space. In particular, in the roll instabilities where n_y and n_z are functions of x, a shear gives rise to a vertical force $F_B = \partial \sigma_{zx} / \partial x$. This *hydrodynamic focusing effect* is responsible for the shear flow instability of the second type and is destabilizing even when the small torque term α_3 is positive and stabilizing.

3. **Experimental.** — The Poiseuille cell was formed by two parallel lucite plates polished to provide the molecular alignment (Fig. 4). Parallel metallic wires of uniform diameter $d = 200\ \mu$ defined the thickness and also limited the parallel flow. Three different widths (D = 8, 5 and 3 mm) were used in the same experiment. Reservoirs at both ends had enough liquid crystal supply to allow a dc flow experiment over several minutes. Two electromagnetic valves triggered electronically were used to apply a given pressure difference Δp in either direction.

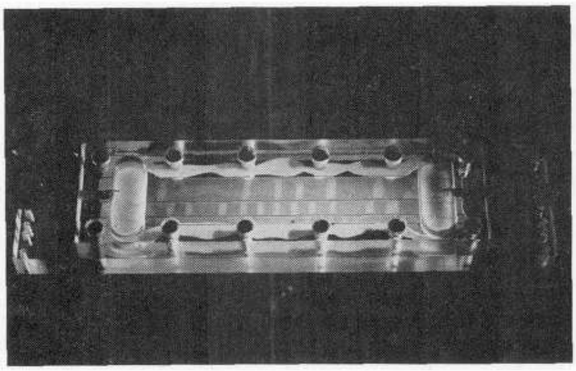

FIG. 4. — The Poiseuille flow cell. The reservoirs at the left and right and the parallel wires separating cells of different widths are visible. The transverse stripes visualize domains of uniform orientation in the homogeneous distorsion mode.

We describe here the results of microscopic visua observations. The wavelength of the roll instabilities was measured from the very regular diffraction pattern of a monochromatic laser beam going through the cell. All observations reported were done after a long enough time was allowed to let the structure stabilize.

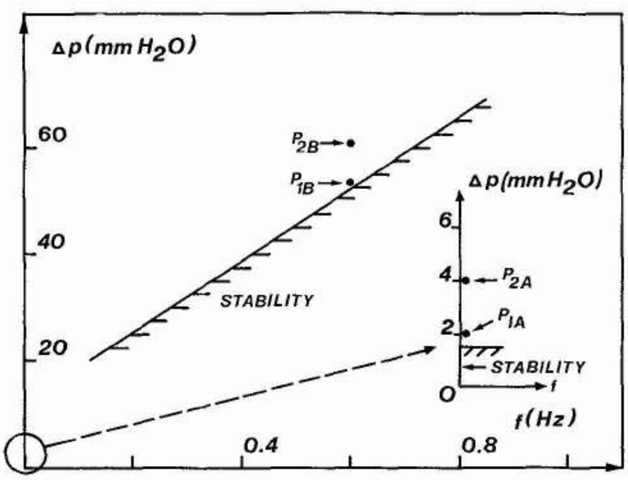

FIG. 5. — The limiting stability curve for large frequencies and in the limit of zero frequency in a diagram where the pressure head Δp is plotted versus the flow frequency $f = T^{-1}$. The points P correspond to instability states discussed in the text.

A given state is characterized by a point on a diagram giving Δp as a function of the frequency T^{-1} of the a. c. flow (Fig. 5) which will be referred to in the following description.

4. **Results and discussion.** — For small enough amplitude flows, the undistorted molecular state is stable. This is in contrast with all other molecular configurations where the distortion appears as soon as there is a flow. We describe different distorted states obtained above a threshold curve which is shown in figure 5 in the limit of zero frequency (d. c. flow) and for flows at large enough frequency. (The intermediate frequency regime is more complex and is not discussed here.)

POINT P_{1A}. — At very low frequencies

$$(T^{-1} = 5 \times 10^{-3}\ \text{Hz})$$

the instability is a uniform distortion in domains limited by boundaries perpendicular to the flow and visible on the photograph of figure 4. The spacing between the domains clearly decreases with the cell width. In the narrowest cell, where the width is of the order of the wall thickness, no domains are obtained. This distortion corresponds to the *homogeneous* shear flow instability : In a given domain the conoscopic image indicates an average twist but no splay as for solution 1 of figure 3. Figure 6 gives a *top* view of the

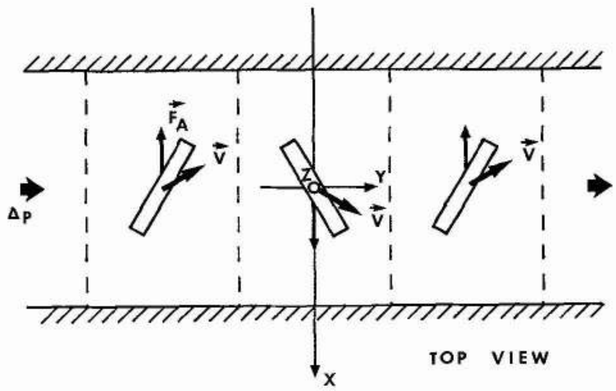

FIG. 6. — Top view of the homogeneous mode. The molecules have an average twist as in solution 1. The transverse force F_A gives rise to a lateral flow velocity v inside each domain. The nature of the flow next to the side wires and in the walls (dotted lines) separating the domains has yet to be studied.

configuration in different domains and points towards the most likely mechanism : As soon as the distortion is present, a transverse force appears, due to the effect A, which deflects the velocity along x. In order to be able to accommodate the transverse flow, domains with opposite transverse velocities develop along the cell. The period of domains is clearly connected with the width of the cell (the nature of the walls, where large shears are present, has not yet been investigated). We call this regime 1 A as it involves solution 1 plus an anisotropic effect of type A.

Although we do not intend to discuss here the threshold problem, an estimate is consistent with the Ericksen number evaluation (2). In a typical experiment with a $L = 8$ cm long cell, $d = 200\ \mu$, the low frequency threshold corresponds to a pressure head $\Delta p_c \sim 2$ mm of water. Using an estimate of $\sqrt{K_1 K_2} \sim 4 \times 10^{-7}$ cgs we get an experimental value $\mathrm{Er}_c \sim 10.9$. The fact that this estimate is lower than the result (2) may be due in part to the transverse flow effects which did not play a role in the shear flow problem but give a first order destabilizing contribution here of magnitude comparable to the ordinary α_3 torque contribution. Only this last effect was evaluated in (2).

Other instability modes with rolls of axis parallel to the flow are seen (Fig. 7). The wavelength of the rolls is independent of the width of the cell and is of the order or smaller than the thickness :

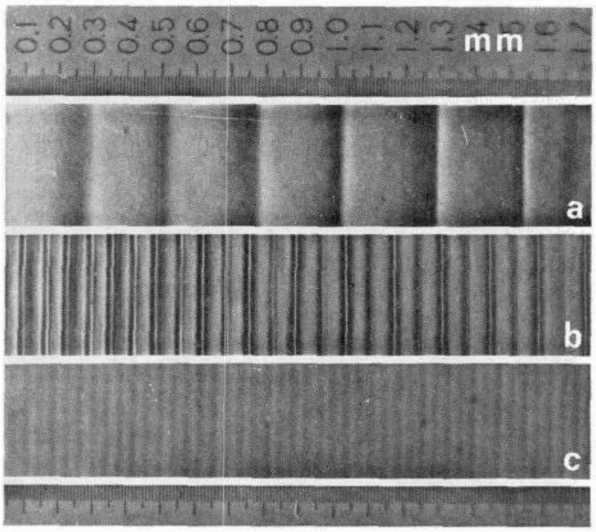

FIG. 7. — A photograph showing, with the same scale, the rolls for the unstable points P_{2A} (*a*), P_{2B} (*b*), P_{1B} (*c*).

POINT P_{1B} (of Fig. 5). — We consider a large frequency (0.5 Hz) flow and a state just above threshold. The observations, in particular the absence of double imaging of dust particles located at the bottom plates, point towards the existence of a solution 1 instability. The dark and light lines (which indicate the lines of maximum curvature of $\mathbf{n}$) along the rolls remain the same when the sign of the flow changed. This shows that the alternating distortion involves a change of sign of n_y and not of the vertical component n_z :

$$n_y(T/2) = -\, n_y(0)$$
$$n_z(T/2) = n_z(0)\,.$$

In the shear flow problem [2] we called this regime a *y mode*. The mechanism for the instability involves a vertical destabilizing *hydrodynamic focusing* force F_B (Fig. 8). This term couples with a vertical hydrodynamic torque which splays the molecules off the *xz* plane.

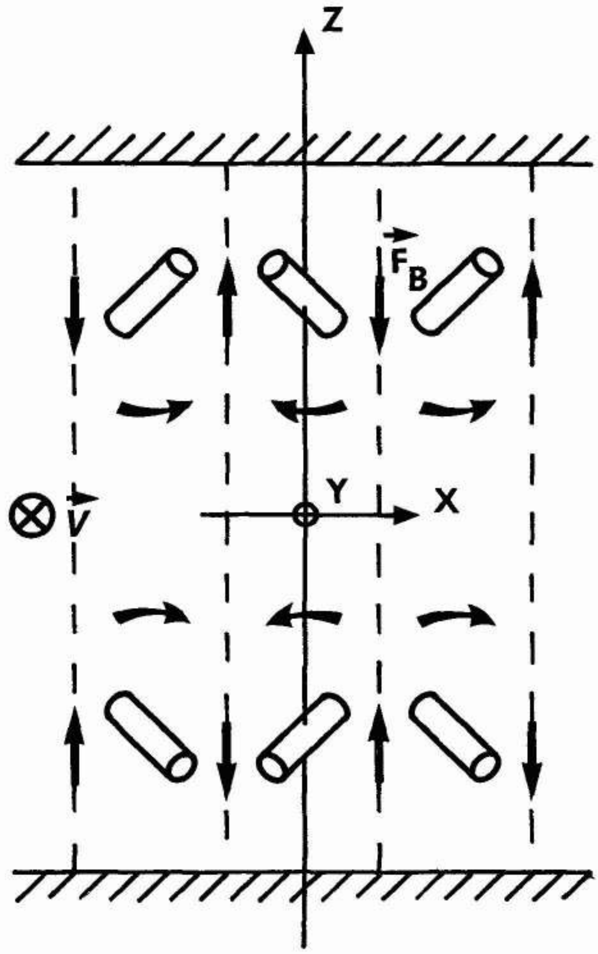

FIG. 8. — (Fig. 8, 10, 11 are viewed along the velocity axis). The proposed distortion corresponds to the linear instability mode taking place at point P_{1B}. The vertical hydrodynamic focusing forces F_{1B} are of opposite signs in both halves of the cell and should cause the formation of two rolls over the cell thickness.

We have characterized the *y* instability mode at point P_{1B} by 1 B (solution 1 plus mechanism B).

Let us note that F_B is of opposite sign in each half of the sample thickness. If, as assumed, F_B induces the formation of convective rolls, *two* rolls should be formed across the cell thickness. The diagram of figure 9 gives the wavelength of the rolls, λ, measured from a laser light beam diffraction pattern, as a function of the pressure head just above threshold. At low frequencies, λ is nearly equal to $d/2$. However, when Δp increases, the wavelength decreases as $\Delta p^{-1/2}$ [9]. This result is clearly understandable : The rolls in both halves of the sample are decoupled. At threshold, the frequency f varies linearly with Δp (see Fig. 5). When f increases, the distortion takes place near the plate over a smaller and smaller thickness of the order of λ such that the elastic time constant for the relaxation of n_y proportional to λ^2 is of the order of f^{-1} (see also formula B 6 and B 7 in reference [2] : when λ decreases, the increase of the hydrodynamic focusing force F_B is compensated by that of the viscous terms in the coupl-

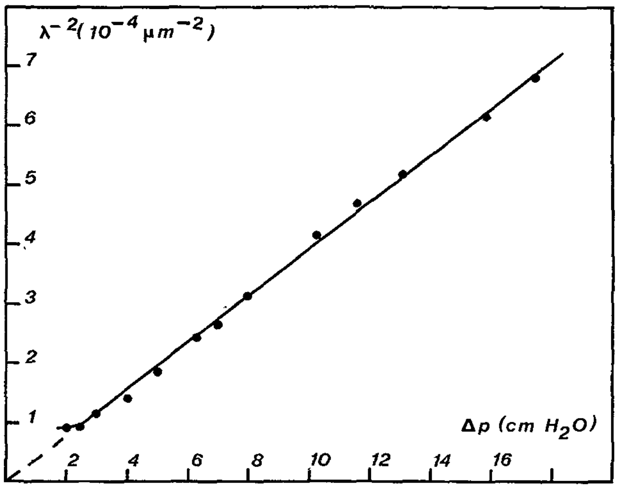

FIG. 9. — The large change of the wavelength λ of the rolls when the pressure head varies just above the stability line of figure 5 could be used for variable wavelength optical grating applications.

ing terms β). The variation of Δp as λ^{-2} can also be obtained directly by considering the expression (2b) for $\mathrm{Er_c}$:

$$\mathrm{Er_c} \propto s_c\,\lambda^2 \propto \Delta p d \lambda^2 .$$

POINT P_{2B}. — *This state corresponds to a relatively* large frequency and a finite amplitude instability. It is quite different from state 1 B. A dust particle gives a double image through the cell. The dark and bright lines of the longitudinal rolls exchange over each half period. The first point indicates a solution of type 2 (finite average splay) whereas the second one is compatible with the *z mode* instability solution described in reference [2] such that

$$n_z(T/2) = -\,n_z(0)$$
$$n_y(T/2) = n_y(0) .$$

Here the vertical distortion oscillates around zero. Again the interpretation (see Fig. 10) involves the destabilizing vertical force F_B ; we characterize this regime as a 2 B mode.

Here, F_B has the same direction for two points on the same vertical in both halves of the cell. Contrarily to the 1 A case, a simple roll formation across the sample is expected. We indeed found that the wavelength of the rolls increased discontinuously going from point P_{1B} to P_{2B} (compare in Fig. 7 the wavelength of the small amplitude rolls (c) to the larger wavelength of the rolls for point P_{1B} (b)).

POINT P_{2A}. — Finally we come back to a state at very low frequency but involving a large enough distortion. The experiments show the existence of rolls parallel to the flow but of wavelength 2 to 3 times the thickness (Fig. 7a). One can check that it is a type 2 solution. A possible explanation of the instability involves the horizontal force due to the anisotropic stress tensor mechanism of type A, the twist of the molecule off the xz plane giving rise to the horizontal force F_A (Fig. 10). There is no sharp distinction between this description and that of figure 9 as in fact F_A and F_B are present at the same time in both cases.

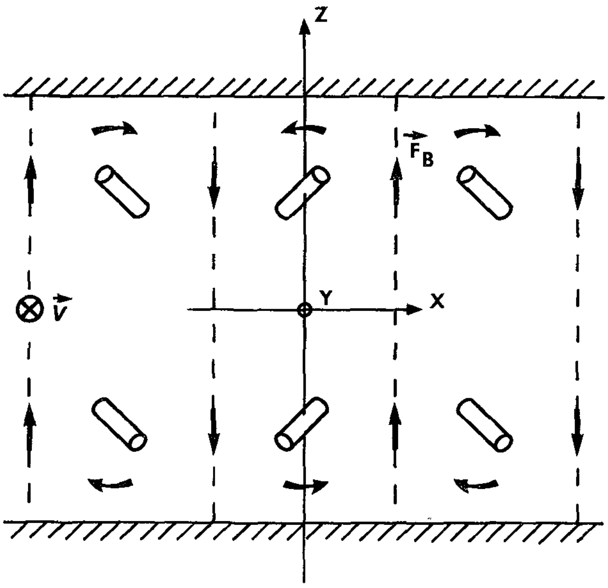

FIG. 10. — Proposed model for the P_{2B} distorted state. Solution 2 is obtained. The vertical force F_B is of the same sign in both halves of the cell.

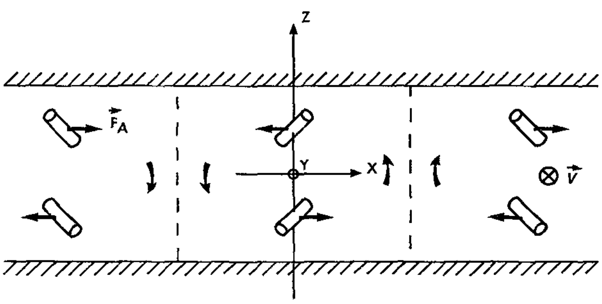

FIG. 11. — Effect of the horizontal transverse force F_A on the type 2 solution. Figures 10 and 11 show two limiting cases for the same type 2 distortion. The analysis of these nonlinear problems is not very clear at present.

We feel that a detailed description of the mechanism at the last two points is probably very difficult, first because it is a finite amplitude problem, secondly because of the coupling of the solutions in both halves of the cell.

More work and in particular quantitative measurements on thresholds is in progress. It is of interest to study the effect of fields. In particular the application of a large enough vertical electric field decreases the elastic time constant for the relaxation of n_z and moves the z mode into the linear instability regime.

Acknowledgments. — We thank P. G. de Gennes for pointing out to us the original features of the Poiseuille flow problem and L. Léger for useful exchanges of information.

Note. — The Poiseuille cell is remarkably simple to assemble and to handle. Then by gently blowing on one end of a tube attached to an end of the cell, one obtains easily the roll structures and the strong decrease of transparence due to *dynamic scattering*. We feel that this simple device should be useful for pedagogical purposes : first, it shows a case of a hydrodynamic instability problem (this is a remarkably simple case, as many hydrodynamic instabilities have only finite amplitude solutions) ; secondly, it provides the most simple demonstration of the coupling between flow and molecular orientation in nematics.

References

[1] PIERANSKI, P. and GUYON, E., *Solid State Commun.* **13** (1973) 435.

[2] PIERANSKI, P. and GUYON, E., *Phys. Rev.* **A 9** (1974) 404.

[3] DE GENNES, P. G., Les Houches *Lectures Notes* (1973). In the problem, Er represents typically the ratio between a time constant associated with the stabilizing elastic effect $\frac{\eta}{K} d^2$ and one due to the destabilizing hydrodynamic mechanism $\frac{\eta}{\alpha s}$. η is a hydrodynamic viscosity.

[4] A comparative description of the mechanism of the shear flow instabilities is given in GUYON, E. and PIERANSKI, P., *Physica* **73** (1974) 184.

[5] GÄHWILLER, Ch., *Mol. Cryst., Liqu. Cryst.* **20** (1973) 301.

[6] We have shown that in materials where $\alpha_2 \alpha_3$ was negative, the homogeneous mode was absent as the small positive torque α_3 had a stabilizing effect ; PIERANSKI, P. and GUYON, E., *Phys. Rev. Lett.* **32** (1974) 924.

[7] PIERANSKI, P. and GUYON, E., *Phys. Lett.* **49A** (1974) 237.

[8] See DE GENNES, P. G., *The Physics of Liquid Crystals* (Oxford University Press) 1974.

[9] This mode provides a remarkably simple and efficient variable wavelength grating which could possibly be used for practical purposes.